Development 136, 2717-2724 (2009) doi:10.1242/dev.038679

β1 integrins are required for normal CNS myelination and promote AKT-dependent myelin outgrowth

Claudia S. Barros[1,*], Tom Nguyen[2,*], Kathryn S. R. Spencer[1], Akiko Nishiyama[3], Holly Colognato[2,†] and Ulrich Müller[1,†]

Oligodendrocytes in the central nervous system (CNS) produce myelin sheaths that insulate axons to ensure fast propagation of action potentials. β1 integrins regulate the myelination of peripheral nerves, but their function during the myelination of axonal tracts in the CNS is unclear. Here we show that genetically modified mice lacking β1 integrins in the CNS present a deficit in myelination but no defects in the development of the oligodendroglial lineage. Instead, in vitro data show that β1 integrins regulate the outgrowth of myelin sheaths. Oligodendrocytes derived from mutant mice are unable to efficiently extend myelin sheets and fail to activate AKT (also known as AKT1), a kinase that is crucial for axonal ensheathment. The inhibition of PTEN, a negative regulator of AKT, or the expression of a constitutively active form of AKT restores myelin outgrowth in cultured β1-deficient oligodendrocytes. Our data suggest that β1 integrins play an instructive role in CNS myelination by promoting myelin wrapping in a process that depends on AKT.

KEY WORDS: β1 integrins, Myelination, Oligodendrocytes, Mouse

INTRODUCTION

In the vertebrate nervous system, myelin sheaths insulate axons and limit membrane depolarization to the nodes of Ranvier, where the machinery propagating action potentials is concentrated (Sherman and Brophy, 2005). Integrins, a family of heterodimeric transmembrane receptors consisting of α and β subunits, are thought to be important for myelination. Integrins containing the β1 subunit are expressed in Schwann cells, the myelinating glial cells of the peripheral nervous system, where they mediate interactions with laminin that are crucial for myelination (Berti et al., 2006). Integrins are also expressed in oligodendrocytes (Milner and ffrench-Constant, 1994; Milner et al., 1997), the myelinating glial cells of the CNS, but less is known about their function in these cells. In vitro studies show that the integrin αvβ1 promotes migration of oligodendrocyte progenitors, whereas α6β1 regulates oligodendrocyte survival and myelin membrane formation in response to laminin 2 (Ln2; Lama2 – Mouse Genome Informatics) (Buttery and ffrench-Constant, 1999; Corley et al., 2001; Frost et al., 1999; Milner et al., 1996; Relvas et al., 2001; Tiwari-Woodruff et al., 2001). Consistent with the in vitro studies, Ln2 is expressed in premyelinating axonal tracts in the CNS, and oligodendrocyte death is increased in the brainstem of mice lacking integrin α6 (Chun et al., 2003; Colognato et al., 2002; Farina et al., 1998; Jones et al., 2001). However, since α6-deficient mice die at birth, it has remained unclear whether the defects in oligodendrocyte survival lead to persistent changes in myelination. In fact, genetic studies addressing the function of β1 integrins in oligodendrocytes have led to contradictory results. Whereas oligodendrocyte-specific expression of a dominant-negative (DN) β1 integrin in a transgenic mouse model was associated with CNS hypomyelination (Camara et al., 2009; Lee et al., 2006), conditional ablation of a floxed allele of the β1 gene (*Itgb1*) in oligodendrocytes using a *CNPase-Cre* (*Cnp-Cre* – Mouse Genome Informatics) driver caused no myelination defects (Benninger et al., 2006). The interpretation of these experiments is complex, as DN β1 integrins can also ectopically activate integrin signaling (Lukashev et al., 1994), and *CNPase-Cre* induces recombination in only a subset of oligodendrocytes by P0 (Benninger et al., 2006).

To circumvent the complications associated with the previous studies, we have analyzed mice in which β1 integrins were inactivated in the ventricular neuroepithelium, including in the oligodendrocyte precursors (referred to here as *Itgb1CNS-ko* mice). We show that in the absence β1 integrins, the thickness of myelin sheets was reduced in axonal tracts in the spinal cord, optic nerves and cerebellum. Defects in myelination were also observed in the spinal cord from mice in which β1 was inactivated solely in NG2 (CSPG4 – Mouse Genome Informatics)-positive oligodendrocyte precursors. Myelination defects were not caused by defects in oligodendrocyte differentiation or survival. Instead, studies with cultured oligodendrocytes show that β1 integrins regulate the outgrowth of myelin sheets. Interestingly, it has recently been shown that overexpression of a constitutively active form of the serine/threonine kinase AKT (AKT1 – Mouse Genome Informatics) in transgenic mice leads to enhanced myelin sheath formation in the CNS without affecting oligodendrocyte proliferation or survival (Flores et al., 2008). We show here that β1 integrins regulate AKT activity in oligodendrocytes, and demonstrate that constitutively active AKT rescues the defect in myelin sheet outgrowth in cultured β1 integrin-deficient oligodendrocytes. Our findings define the role of β1 integrins in CNS myelination and establish a link between β1 integrins and AKT in the control of CNS axonal ensheathment.

[1]The Scripps Research Institute, Department of Cell Biology, Institute of Childhood and Neglected Disease, 10550 N. Torrey Pines Road, La Jolla, CA 92037, USA. [2]Department of Pharmacology, State University of New York, Stony Brook, NY 11794, USA. [3]Department of Physiology and Neurobiology, University of Connecticut, Storrs, CT 06269, USA.

*These authors contributed equally to this work
†Authors for correspondence (e-mails: colognato@pharm.stonybrook.edu; umueller@scripps.edu)

Accepted 11 June 2009

MATERIALS AND METHODS

Mouse lines and western blots

All mouse lines have been previously described (Graus-Porta et al., 2001; Stephens et al., 1995; Zhu et al., 2008). Western blots were carried out as described (Colognato et al., 2002; Graus-Porta et al., 2001). Densitometry and quantification of relative levels of protein expression were performed on scanned images of western blots using MetaMorph software (Universal Imaging). Antibodies used were β1 integrin (Graus-Porta et al., 2001), MBP (Boehringer), PLP (Serotec), actin (Sigma), AKT phospho-S473 and AKT (Cell Signaling).

Oligodendrocyte cultures

Oligodendrocyte progenitors were isolated and cultured following published procedures (Colognato et al., 2007; Colognato et al., 2004), with the addition of a panning step to remove microglia (Cahoy et al., 2008). Briefly, oligodendrocyte progenitor cells (OPCs) were isolated from 10-days-in-vitro (DIV) mixed glial cultures using a 20-hour mechanical dissociation followed by a 30-minute differential adhesion step with uncoated petri dishes. Unattached cells were subjected to two rounds of panning on lectin-coated dishes to remove remaining microglia. Lectin-coated dishes were prepared by incubating petri dishes with 2.3 μg/ml BS-lectin-1 in Dulbecco's PBS (D-PBS) for 4 hours at room temperature, followed by four washes with D-PBS immediately prior to use (Cahoy et al., 2008). Purified OPCs were added to poly-D-lysine (PDL)- or laminin-coated Permanox chamber slides in a modified SATO's medium (SATO with 0.5% FCS for differentiation experiments). Human placental laminin (laminin 211, Sigma) was used to coat the surfaces of slides and dishes at 10 μg/ml in PBS for 4 hours at 37°C. Surface coating with PDL (Sigma) was performed similarly but was instead diluted in dH_2O to obtain 10 μg/ml. Mixed glial cultures from neonatal spinal cords were grown on PDL-coated chamber slides and switched to SATO with 0.5% FCS to differentiate at 10 DIV. Recombinant protein comprising the EGF-like domain of neuregulin 1 was used at 100 ng/ml (PeproTech). The PTEN inhibitor bpV(pic) was used at 31 nM, the IC_{50} for PTEN inhibition (Calbiochem) (Schmid et al., 2004). Wild-type and β1-CNS-mutant mixed glial cultures were transfected using FuGENE (Roche) as described (Colognato et al., 2004), with either MYR-AKT-EGFP or control EGFP plasmids (a kind gift from Dr Bing-Hua Jiang, West Virginia University, Morgantown, WV, USA). Transfected oligodendrocytes were differentiated within the mixed glial cultures and identified 6 days post-transfection using combined GFP and/or MBP immunocytochemistry (see below). A minimum of 25 fields per transfection were evaluated by morphometric analysis.

Electron microscopy and immunochemistry

Electron microscopy (EM) samples were prepared as described (Graus-Porta et al., 2001). EM images were acquired using a Philips CM100 microscope (FEI, Hillsbrough, OR, USA). Morphometric analysis of nerve fibers was performed using MetaMorph software. Immunohistochemistry followed our published procedures (Belvindrah et al., 2007; Blaess et al., 2004). Primary antibodies used were PDGFαR (a kind gift from W. Stallcup, Burnham Institute, La Jolla, CA, USA), CC1 (Calbiotech), OLIG2 (Chemicon) and cleaved caspase 3 (Cell Signaling). Secondary antibodies were Alexa Fluor 488 and 568-conjugated (Molecular Probes). Nuclei were stained with TO-PRO-3 (Molecular Probes). TUNEL assays were carried using the ApopTag Red In Situ Apoptosis Detection Kit (Chemicon). For immunocytochemistry, cells were fixed in 4% PFA (15 minutes) or 100% methanol (5 minutes, –20°C). Blocking and primary antibody incubations were in PBS with 10% donkey serum (with 0.1% Triton X-100 for PFA-fixed cells). Cells undergoing GFP/MBP immunocytochemistry were blocked in PBS with 10% donkey serum and 0.05% Triton X-100. For GALC staining, live cells were labeled with antibody for 30 minutes in DMEM, 1% FCS, followed by washes and PFA fixation. Primary antibodies were NG2 (Chemicon), β1 integrin (Chemicon, MAB1997), GALC (Sigma), CNP (Sigma), MBP (Serotec), GFP (Molecular Probes) and OLIG2 (IBL). Secondary antibodies were FITC- or Texas Red-conjugated (Jackson). Nuclei were stained with DAPI. Images were collected on an Olympus Fluoview 500 confocal microscope, an Olympus AX70 microscope, and a Zeiss Axioplan microscope. MetaMorph software (Universal Imaging) was used for morphometric measures. The AxioVision Interactive Measurement Module was used for myelin sheet and process length cell measures. To ensure consistent analysis across different experiments, MBP-positive cells and MBP-positive sheet-bearing cells were determined using intensity thresholding relative to background intensity (AxioVision). Morphometric analysis to determine the area of coverage of myelin sheets was performed by tracing the outer perimeter of thresholded MBP-positive sheet-bearing oligodendrocytes (AxioVision, Zeiss). Process length measurements were performed on corresponding phase micrographs by tracing from the cell body/process border to the tip of the longest process (AxioVision). Examples of morphometric tracing can be observed in Fig. 7F,G.

Statistical analysis

Statistical analysis was performed using GraphPad Prism. Data show mean ± standard error (mean±s.e.m.). Statistical significance for g-ratio analysis was performed using the Mann-Whitney (rank sum) test. The number of animals analyzed (n) was three unless otherwise indicated. Student's t-test was used for all other assays described. Statistical significance was set at $P<0.05$ (*, significant), $P<0.01$ (**, very significant) and $P<0.001$ (***, highly significant).

RESULTS

CNS myelination defects in *Itgb1-CNSko* and *Itgb1-OL-ko* mice

To define the functions of β1 integrins in CNS myelination, we inactivated β1 expression by crossing mice carrying a floxed integrin β1 gene (*Itgb1-flox*) with nestin-*Cre* mice. In this nestin-*Cre* line, CRE-mediated recombination occurs in neural precursors in the ventricular zone as early as embryonic day (E) 10.5, leading to the inactivation of floxed alleles in developing neurons and glia, including cells at all stages of oligodendrocyte development (Graus-Porta et al., 2001). The mutant mice are viable and fertile and show no obvious behavioral abnormalities (Graus-Porta et al., 2001), and will be referred to as *Itgb1-CNSko* mice (Fig. 1A). We confirmed recombination of the *Itgb1-flox* allele by PCR and the absence of β1 protein by immunoblotting in the spinal cords and brains of mutant mice (Fig. 1B,C; C.S.B., unpublished) (Graus-Porta et al., 2001). In all assays, *Itgb1-CNSko* mice were compared with littermates that did not express CRE but were homozygous for the *Itgb1-flox* allele or carried one *Itgb1-flox* and one *Itgb1-null* allele. Control mice are referred to as wild type (WT) because previous studies revealed that the loxP sites or heterozygosity for *Itgb1-null* do not affect β1 function (Graus-Porta et al., 2001; Stephens et al., 1995). Histological analysis showed that spinal cords from *Itgb1-CNSko* adult mice were not obviously different in overall morphology from WT (Fig. 1D).

To examine myelin sheaths in *Itgb1-CNSko* mice, we analyzed spinal cords by electron microscopy (EM). The amount of myelin sheath insulating axons increases in proportion to the axon diameter (Sherman and Brophy, 2005). In *Itgb1-CNSko* mutants, the thickness of myelin surrounding axons was reduced compared with WT (Fig. 2A). Morphometric analysis of the nerve fibers revealed a significant increase in the ratio of axon diameter to fiber diameter (g-ratio; Fig. 2B; see Table S1 in the supplementary material). Interestingly, the smallest caliber axons (of <0.7 μm diameter) did not show decreases in myelin thickness (Fig. 2B; see Table S1 in the supplementary material). The periodicity of myelin sheets in the mutants was unaffected, suggesting that the overall reduction in myelin thickness resulted from a decrease in the number of wraps (insets in Fig. 2A, lower panels). We also observed no axonal swelling or degeneration, and no changes in the density or size of axons (Fig. 2A,C,D). Consistent with myelination defects, the levels of two major CNS myelin components, myelin basic protein (MBP)

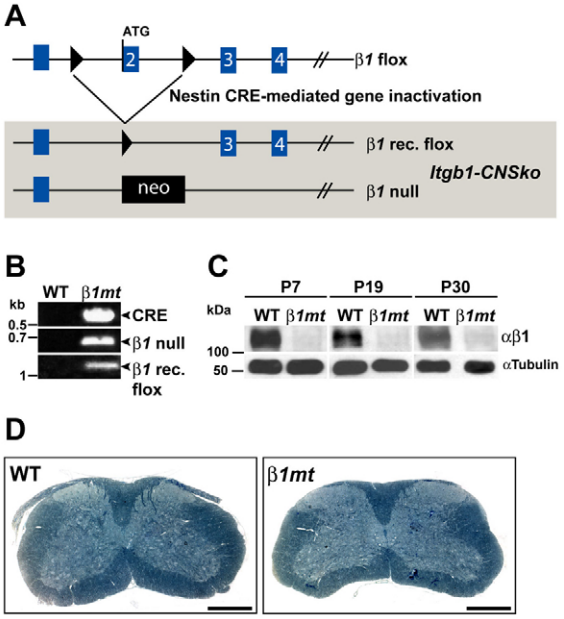

Fig. 1. CRE-mediated gene inactivation leads to loss of β1 integrin protein. (**A**) Diagram of nestin-*Cre*-mediated gene inactivation in *Itgb1-CNSko* mice mutants. The *Itgb1* (encodes β1 integrin) floxed allele before and after recombination (rec) and the *Itgb1-null* allele are shown. LoxP sites are indicated as black triangles, exons (blue boxes) are numbered. *neo* indicates neomycin cassette. (**B**) DNA from the P19 spinal cord of WT and *Itgb1-CNSko* mice (*β1mt*) was analyzed by PCR. With DNA from *Itgb1-CNSko* mice, bands corresponding to the nestin-*Cre* transgene, the *Itgb1-null* allele and the recombined *Itgb1-flox* allele were detected. (**C**) Immunoblotting with β1 integrin antibody using spinal cord extracts from mice at P7, P19 and P30 showed loss of β1 protein in the mutants. Tubulin served as a loading control. (**D**) Spinal cord sections from WT and *Itgb1-CNSko* mice at P30 stained with Toluidine Blue. No obvious differences in overall morphology were detected. Scale bar: 500 μm.

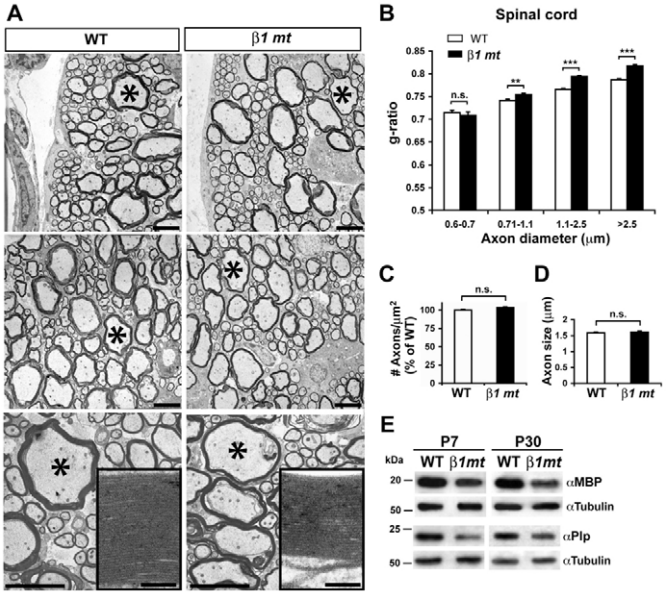

Fig. 2. Myelination defects in the spinal cords of *Itgb1-CNSko* mutants. (**A**) Electron microscopy (EM) analysis of myelinated fibers in spinal cord sections from P30 *Itgb1-CNSko* and WT mice. Asterisks indicate axons of similar size. Insets in lower panels show higher magnifications of myelin wraps from indicated axons. Scale bars: 5 μm; 100 nm for insets in lower panels. (**B**) G-ratio (axon diameter/fiber diameter) of fibers grouped by axon diameter. Values are shown as mean±s.e.m. In *Itgb1-CNSko* mutants, the g-ratio was significantly increased, with the exception of axons with a diameter less than 0.7 μm. See Table S1 in the supplementary material for statistical values. (**C**,**D**) No significant change was detected in either the density (C) or size (diameter, D) of axons in *Itgb1-CNSko* mutants [density: *β1mt* 0.101±0.01/μm^2 (103.52±1.14% with respect to WT), WT 0.097±0.01/μm^2, P>0.05, n=1660 axons from three WT, n=2009 axons from three *Itgb1-CNSko* mutants; size (diameter): *β1mt* 1.61±0.03 μm, WT 1.59±0.03 μm, P>0.05, n=1660 axons from three WT, n=2009 axons from three *Itgb1-CNSko* mutants]. Values are shown as mean±s.e.m. (**E**) Immunobloting for MBP and PLP in spinal cord extracts from P7 and P30 *Itgb1-CNSko* mutant and WT mice. Tubulin served as a control for loading and subsequent densitometry analysis. In mutant spinal cords at P7, the relative levels of MBP and PLP proteins were reduced by 23.1±2.5% (n=3, ***P<0.001) and 24.9±6.8% (n=3, *P<0.05), respectively. At P30, MBP and PLP levels were decreased in mutant spinal cords by 36.5±12.1% (n=3, *P<0.05) and 13.5±3% (n=2, *P<0.05), respectively. n.s., not significant.

and proteolipid protein (PLP, PLP1 – Mouse Genome Informatics) (Simons and Trajkovic, 2006), were modestly but significantly reduced in *Itgb1-CNSko* mice (Fig. 2E).

To investigate whether other axonal tracts in the CNS were similarly affected, we analyzed the optic nerves and the cerebellum. As in the spinal cord, myelin sheaths enwrapping the larger caliber axons were reduced in thickness (Fig. 3A,B; see Table S1 in the supplementary material). We also attempted to analyze myelination in the corpus callosum, but its organization was significantly disrupted in *Itgb1-CNSko* mice due to the perturbations in cortical size and structure (Graus-Porta et al., 2001), preventing a meaningful analysis.

To determine the extent to which β1 integrins in oligodendroglia are required for myelination, we inactivated their expression using *Ng2-Cre* mice. In this mouse line, CRE specifically induces the recombination of floxed alleles in NG2-positive oligodendrocyte precursors (Zhu et al., 2008). The analysis of axonal tracts in the spinal cord of these mutants (named *Itgb1-OL-ko* mice) revealed a reduction in myelin thickness (Fig. 4A,B). As in *Itgb1-CNSko* mice, myelin thickness was affected in axons with diameters >0.7 μm, although the phenotype was less severe, and some of the largest diameter axons appeared unaffected (Fig. 4C). The less severe defect in myelination could be a consequence of less effective inactivation of β1 integrins by *Ng2-Cre* compared with nestin-*Cre*. To test this hypothesis, we purified oligodendrocytes from mutant mice and analyzed integrin expression by immunohistochemistry and western blotting. Staining for NG2 and OLIG2 confirmed that oligodendrocytes were purified to near homogeneity (see Fig. S1A-C in the supplementary material). Whereas β1 integrins were almost completely absent in oligodendrocytes from *Itgb1-CNSko* mice (Fig. 6A,B,I), a low amount of β1 integrin expression could still be detected in oligodendrocytes from *Itgb1-OL-ko* mice (see Fig. S1D,E in the supplementary material), suggesting that the less severe myelination defect in *Itgb1-OL-ko* mice was a consequence of less efficient CRE-mediated recombination. However, it cannot be excluded that β1 integrins in axons, which were inactivated by nestin-*Cre* but not by *Ng2-Cre*, also contributed to myelination. Taken together, our findings demonstrate that β1 integrins are

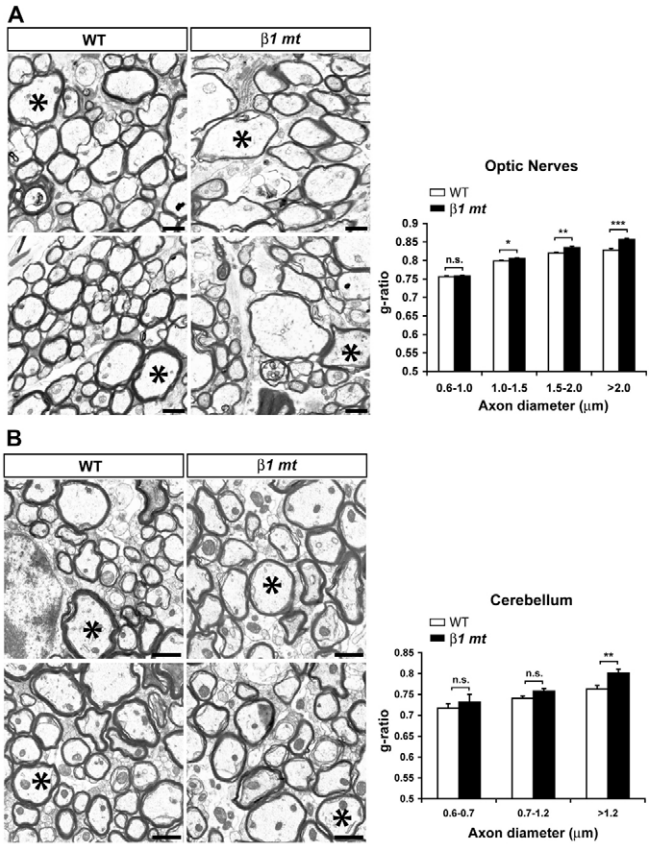

Fig. 3. Myelination defects in the optic nerves and cerebellum of *Itgb1-CNSko* mutants. (**A**,**B**) EM analysis of myelinated fibers in optic nerve (A) and cerebellum (B) cross-sections from P30 *Itgb1-CNSko* and WT mice. Asterisks indicate axons of similar size. The g-ratios (diameter axon/diameter fiber) of fibers grouped by axon diameter are also shown (mean±s.e.m.). In *Itgb1-CNSko* mutant optic nerves and cerebellum there was an increase in the g-ratio of fibers with larger axonal calibers compared with WT. See Table S1 in the supplementary material for statistical data. n.s., not significant. Scale bars: 1 μm.

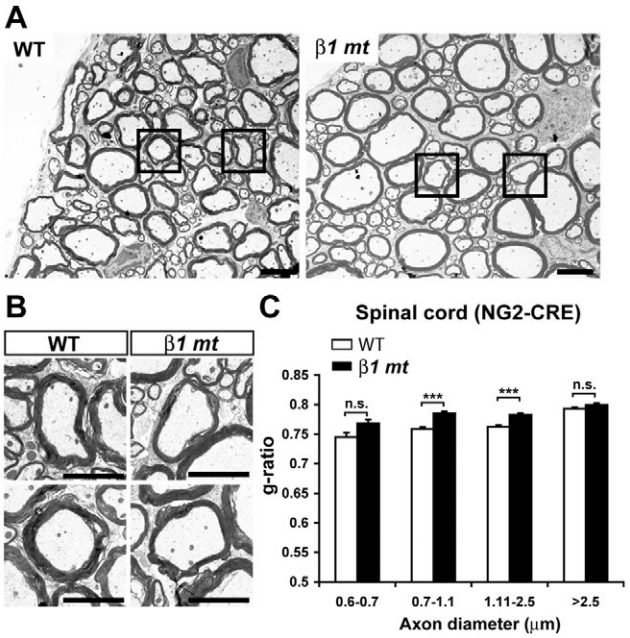

Fig. 4. Myelination defects in the spinal cords of *Itgb1-OL-ko* mutants derived using *Ng2-Cre*. (**A**) EM analysis of myelinated fibers in spinal cord sections from P30 *Itgb1-OL-ko* and WT mice generated using the *Ng2-Cre* driver. (**B**) Higher magnification of fibers boxed in A. (**C**) G-ratio of fibers grouped by axon diameter (mean±s.e.m.). In *Itgb1-OL-ko* mutants, the g-ratio was significantly increased in axons with a diameter between 0.7 and 2.5 μm. n.s., not significant. See Table S1 in the supplementary material for statistical values. Scale bars: 5 μm in A; 2.5 μm in B.

required for the myelination of axonal tracts in the spinal cord, optic nerve and cerebellum, and that they act, at least in part, in oligodendrocytes to carry out their function.

Oligodendrocyte lineage development in *Itgb1-CNSko* mutants

The hypomyelination of axonal tracts in the CNS of *Itgb1-CNSko* mutants could arise from defects in oligodendrocyte development. We therefore analyzed their development using stage-specific molecular markers. The number of PDGFαR-positive oligodendrocyte progenitors at postnatal day (P) 0, prior to axonal ensheathment, was not reduced in the mutants (Fig. 5A,B,G; *β1mt* 17.88±1.09/μm^2, WT 17.95±1.21/μm^2, P>0.05, n=3). Similarly, there was no reduction in the numbers of CC1-positive oligodendrocytes at P19, when myelination is in progress (Fig. 5C,D,H; *β1mt* 32.71±0.89/μm^2, WT 33.5±1.36/μm^2, P>0.05, n=3), or at P60, after myelin sheaths have formed (Fig. 5E,F,H; *β1mt* 34.17±1.05/μm^2, WT 34.89±0.78/μm^2, P>0.05, n=3). Detection of OLIG2, which labels oligodendroglia throughout their development, also revealed no defects in mutant animals (see Fig. S2 in the supplementary material). Finally, we analyzed cell death in the mutants and observed no differences in either the developing or adult spinal cords (see Fig. S3 in the supplementary material). Analysis of the developing cerebellum also revealed no significant increase in the numbers of dying cells (see Fig. S4 in the supplementary material). We conclude that the reduction in myelin ensheathment in *Itb1-CNSko* mice is probably not caused by the loss of oligodendrocytes.

To further define the cell-autonomous function of β1 integrins in oligodendrocytes, we purified their progenitors from WT and *Itgb1-CNSko* mice to near homogeneity (see Fig. S1A-C in the supplementary material) and followed their differentiation in vitro (Fig. 6). Immunostaining and western blots confirmed the efficient inactivation of β1 integrins in oligodendrocytes from *Itgb1-CNSko* mice (Fig. 6A,B,I). The percentage of NG2-positive oligodendrocyte precursors that were present 1 day after plating into differentiation medium was not significantly different between WT and β1-deficient cells (Fig. 6C,D,J; *β1mt* 46.83±3.02%, WT 50.90±5.32%, n=4, P>0.05). No difference was observed in the percentage of GALC-positive oligodendrocytes at days 2 or 4 (Fig. 6E,F,K; *β1mt* 67.05±2.1%, WT 66.89±3.72%, n=4, P>0.05 at day 2; *β1mt* 81.6±2.82%, WT 78.87±4.29%, n=4, P>0.05 at day 4), or MBP-positive mature oligodendrocytes at 4 or 6 days postplating in differentiation medium (Fig. 6G,H,L; *β1mt* 33.26±4.37%, WT 37.39±4.54%, n=4, P>0.05 at day 4; *β1mt* 23.28±2.95%, WT 32.97±4.22%, n=4, P>0.05 at day 6). These data are in agreement with our in vivo analysis (Fig. 5; see Fig. S2 in the supplementary material) and confirm that β1 integrins are not essential for the formation of mature oligodendrocytes.

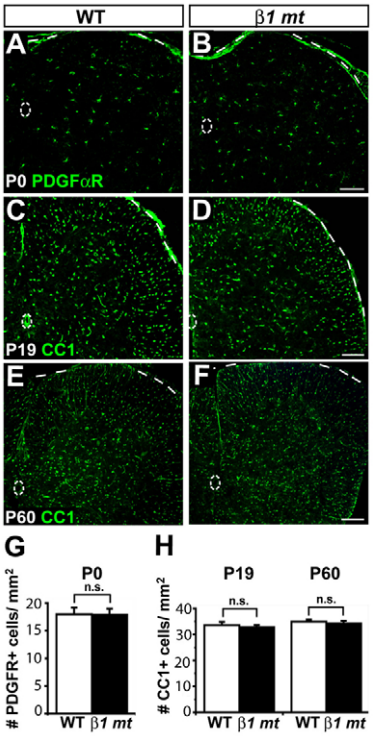

Fig. 5. Normal oligodendrocyte lineage progression in *Itgb1-CNSko* mice. (**A-F**) Spinal cord cross-sections from *Itgb1-CNSko* and WT mice immunostained with antibodies against the oligodendrocyte progenitor marker PDGFαR (green) at P0 and the mature oligodendrocyte marker APC at P19 and P60 (CC1 antibody, green). Dashed lines mark spinal cord borders and central canal. Scale bars: 100 μm. (**G**,**H**) Cell density quantifications (mean±s.e.m.) showed no significant decrease (n.s.) in the numbers of PDGFαR (G)- or CC1 (H)-positive cells in *Itgb1-CNSko* mutants.

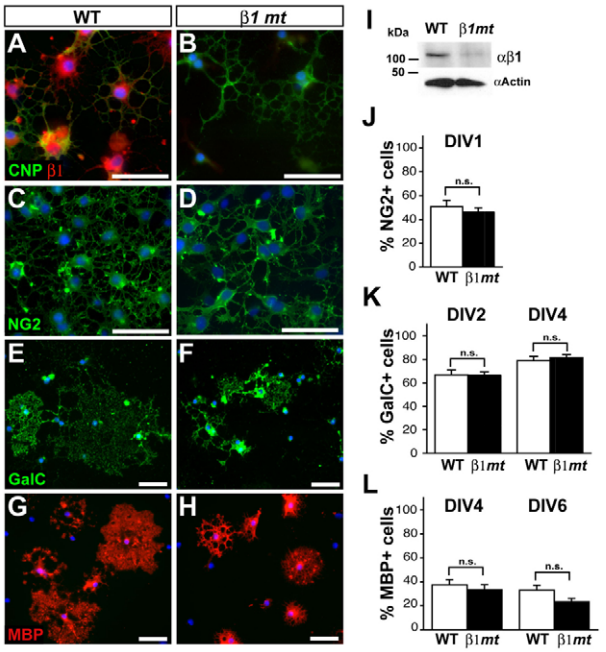

Fig. 6. Normal lineage progression in cultured *Itgb1-CNSko*-derived oligodendrocytes. Oligodendrocyte progenitors obtained from *Itgb1-CNSko* or WT brains were differentiated for 1, 2, 4 or 6 days in vitro (DIV). Immunocytochemistry was used to visualize the oligodendroglia marker CNP (green) and β1 integrin (red) at 2 DIV (**A**,**B**), the oligodendrocyte progenitor marker NG2 (green) at 1 DIV (**C**,**D**), the premyelinating oligodendrocyte marker GALC (green) at 4 DIV (**E**,**F**) and the mature oligodendrocyte marker MBP (red) at 4 DIV (**G**,**H**). All images show counterstaining with DAPI to visualize nuclei (blue). Scale bars: 50 μm. (**I**) Western blot analysis of lysates obtained from oligodendrocytes purified from wild-type and *Itgb1-CNSko* mice revealed a severe reduction in the levels of β1 integrin protein in mutant cells (*β1mt*). Actin blots were performed as a loading control. (**J-L**) Quantification of the percentage of cells expressing NG2 at 1 DIV (J); GALC at 2 and 4 DIV (K); and MBP at 4 and 6 DIV (L) revealed no differences between *Itgb1-CNSko*- and WT-derived cells. Values are shown as mean±s.e.m. n.s., not significant.

Defects in myelin sheet outgrowth in β1-deficient oligodendrocytes

Myelin membrane sheets are formed by the extension of branched processes surrounded by a specialized plasma membrane enriched with myelin proteins such as MBP (Richardson et al., 2006). Myelin membrane sheet formation is therefore thought to mimic many of the morphological changes that take place during oligodendrocyte ensheathment of axons (Simons and Trotter, 2007). While performing lineage analysis, we observed that MBP-positive oligodendrocytes derived from the cerebral cortex of *Itgb1-CNSko* mutants extended smaller myelin membrane sheets (Fig. 6G,H and Fig. 7A). Morphometric analysis further revealed that fewer mutant oligodendrocytes elaborated myelin membrane sheets (Fig. 7B; *β1mt* 29.98±1.81%, WT 36.62±0.23%, n=4, P<0.05 at day 2), and that the β1-deficient sheets were significantly smaller than their WT counterparts (Fig. 7C; *β1mt* 2409.12±225.79 μm^2, WT 4164.7±311.60 μm^2, n=4, P<0.05 at day 2; *β1mt* 3658.04±457.05 μm^2, WT 5557.27±806.51 μm^2, n=4, P<0.05 at day 4). The decrease in sheet outgrowth was also reflected by a decrease in the mean length of mutant oligodendrocyte processes (Fig. 7D; *β1mt* 85.01±5.59 μm, WT 115.16±3.16 μm, n=4, P<0.05 at day 4).

To confirm that defects in the formation of myelin sheets were not confined to oligodendrocytes from the cerebral cortex, we evaluated mixed glial cultures from the spinal cord. Examples for the morphometric analysis to determine MBP sheet area and process length are shown in Fig. 7F,G. Spinal cord oligodendrocytes from WT and mutant mice on average elaborated larger membrane sheets than those prepared from cerebral cortices. However, sheets formed by β1-deficient spinal cord oligodendrocytes were significantly smaller than those from WT controls (Fig. 7E; *β1mt* 9863.98±719.86 μm^2, WT 12,944.54±346.64 μm^2, n=4, P<0.05).

Activated AKT mediates β1 integrin function in myelin sheet outgrowth

Several signaling molecules have been implicated in controlling myelination, including the serine/threonine kinase AKT (Flores et al., 2008). To determine whether β1-deficient oligodendrocytes exhibited defects in AKT activation, we plated oligodendrocytes on laminin and treated the cultures with neuregulin 1 to stimulate AKT phosphorylation (Fig. 8A). We made use of neuregulin 1 because integrin signaling in oligodendrocytes amplifies receptor tyrosine kinase signaling, where neuregulin 1 signaling is particularly sensitive to integrin engagement (Colognato et al., 2002; Colognato et al., 2004). Whereas WT oligodendrocytes showed a large increase in AKT phosphorylation at serine 473 (211±48.29% compared with

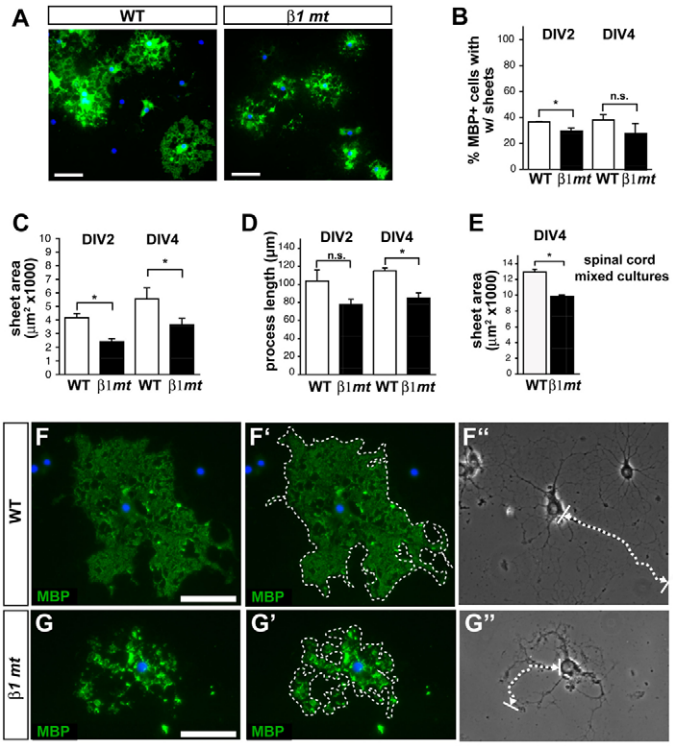

Fig. 7. *Itgb1-CNSko* oligodendrocytes have smaller myelin membrane sheets. (**A**) Oligodendrocytes derived from WT and *Itgb1-CNSko* mice were differentiated for 4 DIV, then visualized using MBP immunocytochemistry (green) and counterstained with DAPI (blue). (**B**) Percentage of MBP-positive oligodendrocytes containing visible sheet-like morphology at 2 and 4 DIV. Values are shown as mean±s.e.m. At 2 DIV, β1-deficient oligodendrocytes contained significantly fewer sheets than WT counterparts (**P*<0.05). The difference was not significant (n.s.) at 4 DIV. (**C**) The mean area of MBP-positive myelin membranes (mean±s.e.m.) was smaller in β1-deficient oligodendrocytes at 2 and 4 DIV (**P*<0.05). (**D**) The length of the longest process within each myelin membrane sheet (mean±s.e.m.) was significantly shorter in mutant oligodendrocytes at 4 DIV (**P*<0.05). (**E**) The area of MBP-positive myelin sheets (mean±s.e.m.) was compared with mixed glial cultures obtained from WT or *Itgb1-CNSko* spinal cords at P0. Spinal cord oligodendrocytes from mutant mice generated smaller myelin membrane sheets at 4 DIV (**P*<0.05). (**F-G″**) Representative pictures depicting morphometric analysis performed on MBP-positive (green) wild-type (F-F″) and β1 mutant (G-G″) oligodendrocytes. Scale bars: 50 μm.

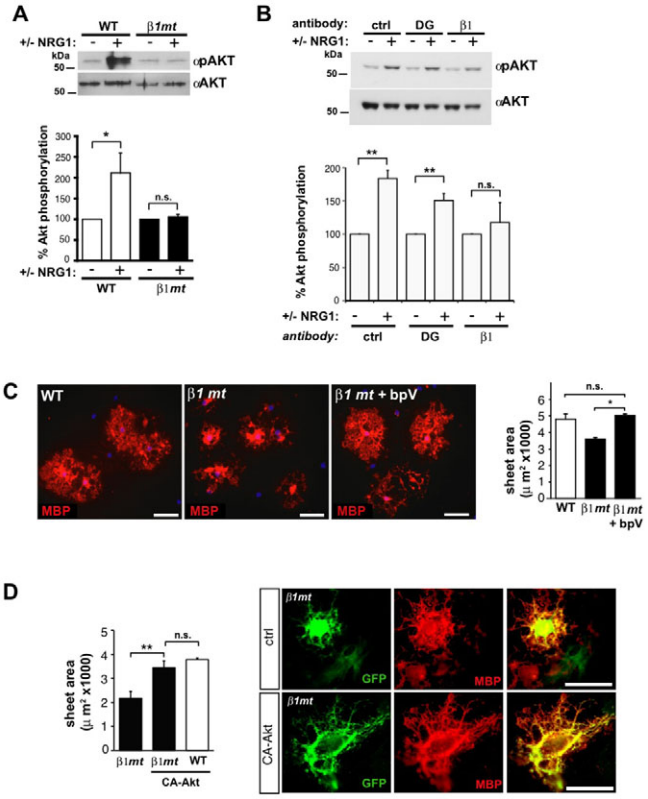

Fig. 8. β1 integrin function in myelin sheet outgrowth is mediated by AKT. (**A**) Oligodendrocytes derived from either from WT or *Itgb1-CNSko* brains were cultured on laminin and stimulated with neuregulin 1 (NRG1) at 1 DIV and evaluated by western blot to detect pAKT (phospho-Ser473) and total AKT. Densitometry of western blots is also shown. Only WT oligodendrocytes showed an increase in relative AKT phosphorylation (ratio of pAKT/total AKT) upon stimulation (mean±s.e.m.; **P*<0.05). (**B**) Wild-type rat oligodendrocytes were treated with control (ctrl), dystroglycan (DG)- or β1-integrin-blocking antibodies followed by stimulation with neuregulin 1 (NRG1) at 1 DIV. Cells were lysed and evaluated by western blot to detect pAKT (phospho-Ser473) and total AKT. Densitometry of blots is also shown. Cells treated with control or dystroglycan-blocking antibodies, but not β1-integrin-blocking antibodies, showed a significant increase in relative AKT phosphorylation (ratio of pAKT/total AKT) upon stimulation (mean±s.e.m.; ***P*<0.01). (**C**) WT and β1-deficient oligodendrocytes differentiated for 4 DIV in the presence or absence of the PTEN inhibitor bpV were visualized using MBP antibody (red) and counterstained with DAPI (blue). The area of MBP-positive myelin sheets after 4 DIV in the presence or absence of bpV (mean±s.e.m.) was calculated. Mutant oligodendrocytes showed sheets of WT size after treatment with bpV (**P*<0.05). (**D**) WT and β1-deficient mixed glial cells were transfected with either CA-AKT-GFP or control GFP constructs and evaluated by immunocytochemistry to monitor construct expression (GFP, green) and MBP-positive myelin membrane (MBP, red). The area of MBP-positive myelin sheets in the presence of CA-AKT or control GFP is shown (mean±s.e.m.). Mutant oligodendrocytes transfected with CA-AKT showed sheets significantly larger than mutant oligodendrocytes transfected with control GFP (***P*<0.01). Scale bars: 50 μm.

untreated WT, n=8, P<0.05), β1-deficient oligodendrocytes did not show significant AKT activation (105.78±6.15% compared with untreated *β1mt*, n=8, P>0.05). Oligodendrocytes grown on control poly-D-lysine substrates showed low levels of AKT phosphorylation that were not significantly different between WT and mutants (see Fig. S5A in the supplementary material). In addition, a similar AKT stimulation assay was performed using β1-integrin-blocking antibodies on wild-type rat oligodendrocytes grown on laminin (Fig. 8B). Oligodendrocyte progenitor cells were attached for 2 hours, followed by differentiation for 22 hours in the presence of β1-integrin-blocking antibodies. Cells were treated with neuregulin for 30 minutes and AKT phosphorylation was evaluated (Fig. 8B). Neuregulin-treated oligodendrocytes showed a significant increase in AKT phosphorylation in the presence of the control antibody (183.52±12.03%, n=4, P<0.01), whereas cells treated with β1-integrin-blocking antibodies showed no significant increase (117.54±29.87%, n=4). To ascertain β1 integrin specificity, we also used antibodies that block the non-integrin laminin receptor dystroglycan, which is expressed in oligodendrocytes (Colognato et

al., 2007). In the presence of the dystroglycan antibody, AKT phosphorylation was still significantly activated by neuregulin 1 (150.65±10.25%, n=4, P<0.01). Thus, loss of β1 integrin protein (Fig. 8A) and function (Fig. 8B) affects the ability of oligodendrocytes to activate signaling pathways leading to AKT phosphorylation.

We next sought to investigate whether the defects in myelin sheet outgrowth in β1-deficient oligodendrocytes could be attenuated upon increased activation of AKT. Strikingly, treatment with a PTEN inhibitor (bpV) to enhance AKT phosphorylation caused mutant oligodendrocytes to grow myelin membrane sheets of an equivalent size to WT (Fig. 8C; *β1mt* + bpV 5026.72±90.34 μm^2 versus *β1mt* untreated 3612.06±97.31 μm^2, n=4, P>0.05; *β1mt* + bpV 5026.72±90.34 μm^2 versus WT 4800.85±312.75 μm^2, n=4, P<0.05). WT myelin membrane sheets, however, did not become significantly larger in the presence of the PTEN inhibitor (see Fig. S5B in the supplementary material). To determine more directly whether AKT signaling can rescue the defect in myelin sheets in β1-deficient oligodendrocytes, we transfected them with a construct expressing a constitutively active AKT-GFP fusion protein (CA-AKT) or with control GFP (Fig. 8D). Transfected oligodendrocytes were visualized by staining for GFP and MBP and the membrane sheet area was determined. The expression of CA-AKT dramatically increased the myelin sheet area in β1 mutant oligodendrocytes and restored it to near wild-type levels (Fig. 8D; *β1mt* + control GFP 2174.65±280.15 μm^2 versus *β1mt* + CA-AKT 3449.05±274.46 μm^2; WT + CA-AKT 3783.54±69.66 μm^2; n=2, P<0.01). Collectively, these results suggest that β1 integrins are required for the regulation of AKT activity, and that defects in this process contribute to the abnormal myelin outgrowth observed in β1-deficient oligodendrocytes.

DISCUSSION

We show here that β1 integrins are required for the myelination of axonal tracts in the CNS and we establish a link between β1 integrins and AKT in oligodendrocyte function. Myelin thickness was reduced in the spinal cord, cerebellum and optic nerve of *Itgb1-CNSko* mice without a reduction in oligodendrocyte numbers. These findings suggest that the myelination defects in mutant mice were caused by perturbations in the formation of myelin membrane sheaths. Consistent with this finding, myelin outgrowth was substantially impaired in cultured β1-deficient oligodendrocytes. Myelination was also affected in the spinal cord of *Itgb1-OL-ko* mice, providing additional evidence that β1 integrins act, at least in part, cell-autonomously in oligodendrocytes to regulate myelination. Interestingly, activation of AKT signaling was affected in cultured β1-deficient oligodendrocytes. Furthermore, myelin membrane sheet formation in the β1-mutant cultured cells was restored by inhibiting PTEN or by overexpressing constitutively active AKT. Taken together, these findings provide strong evidence that AKT is crucial for β1 integrin function during the myelination of axonal tracts in the CNS.

Previous studies have provided conflicting results regarding the function of β1 integrins in CNS myelination. Although the expression of a dominant-negative β1 integrin in oligodendrocytes has been reported to affect myelination (Camara et al., 2009; Lee et al., 2006), no such defect was observed in mice following β1 integrin inactivation in oligodendrocytes using *CNPase-Cre* (Benninger et al., 2006). We now report significant defects in CNS myelination in mice when β1 integrins are inactivated with nestin-*Cre*, supporting the view that β1 integrins are important for CNS myelination. In addition, we observed defects in myelination in *Itgb1-OL-ko* mice, in which integrins have been inactivated in oligodendrocytes using *Ng2-Cre*. We consider it likely that the differences in the results reported here and the earlier study (Benninger et al., 2006) can be explained by differences in the efficiency and timing of CRE expression. CNP is expressed relatively late during oligodendrocyte differentiation (Scherer et al., 1994), and CNP-CRE induces recombination in ~65% of oligodendrocytes at around P0 (Benninger et al., 2006). By contrast, NG2 is already expressed in oligodendrocyte precursors at the stage when PDGFαR is expressed (Nishiyama et al., 1996), which is a marker for the earliest stages of oligodendrocyte differentiation. NG2-CRE has also been reported to lead to recombination in approximately 90% of NG2-positive cells (Zhu et al., 2008). Since oligodendrocytes are generated in excess (Raff et al., 1998), sufficient progenitors probably escaped gene inactivation and were able to compensate for the loss of β1 integrin protein in some progenitors. Interestingly, myelination defects in *Itgb1-CNSko* mice were more severe than in *Itgb1-OL-ko* mice. As β1 integrins in *Itgb1-CNSko* mice were inactivated in both neurons and oligodendrocytes, β1 integrins in axons might have additional roles in myelination.

We provide here insights into the mechanisms by which β1 integrins regulate myelination in the CNS. Unlike in previous studies, which indicated that β1 integrins regulate oligodendrocyte survival (Benninger et al., 2006; Colognato et al., 2002; Lee et al., 2006), we only detected a small trend towards increased death in the developing cerebellum of *Itgb1-CNSko* mice. Although we cannot fully explain the difference with previous studies, our findings suggest that the subtle changes in oligodendrocyte death in *Itgb1-CNSko* mice were compensated for during development. The changes in myelin thickness that we observed are therefore probably not caused by a decrease in the number of oligodendrocytes but by defects in myelin membrane outgrowth. This interpretation is consistent with our in vitro data, which demonstrate that the formation of myelin membrane sheets was affected in β1-deficient cultured oligodendrocytes.

Interestingly, recent findings show that constitutively active AKT enhances myelination without affecting the number of oligodendrocytes (Flores et al., 2008). Mice lacking the P85α regulatory subunit (PIK3R1 – Mouse Genome Informatics) of PI3K, an activator of AKT, show hypomyelination in the CNS (Tohda et al., 2007), whereas knockout mice for PTEN, a negative regulator of PI3K/AKT signaling (Sulis and Parsons, 2003), have thickened CNS myelin sheaths (Fraser et al., 2008). The opposite effects of β1 inactivation and AKT activation on myelination prompted us to test whether the two proteins are functionally linked. Consistent with this model, the loss of β1 integrins in oligodendrocytes affected AKT activation. A second laminin receptor, dystroglycan, which also promotes myelin membrane outgrowth in vitro (Colognato et al., 2007), did not affect AKT activation, indicating that there is a specific link between AKT and β1 integrins. Furthermore, defects in myelin membrane outgrowth in β1-deficient oligodendrocytes were rescued upon expression of constitutively active AKT or by modulating endogenous AKT activity levels with a PTEN inhibitor. Based on these findings, we suggest that β1-deficient oligodendrocytes are unable to properly myelinate axons at least in part due to defective AKT signaling. Interestingly, focal adhesion kinase (FAK, PTK2 – Mouse Genome Informatics) and integrin linked kinase (ILK), mediators of integrin functions that control AKT, have also been implicated in the regulation of myelin sheet outgrowth by oligodendrocytes (Chun et al., 2003; Hoshina et al., 2007). Collectively, these data support a model in which

extracellular ligands that activate β1 integrins induce AKT activity to control myelin outgrowth and axonal wrapping in the CNS. In the future, it will be important to define the downstream effectors of AKT and the extent to which they integrate biosynthetic and cytoskeletal pathways to control the outgrowth of myelin membranes that enwrap axonal processes in the CNS.

Acknowledgements
We thank T. Bossing for critical reading of the manuscript; M. Wood for EM technical support; D. Park for technical support; and Dr Bian-Hua Jiang for the generous gift of MYR-AKT-GFP. This work was supported by funding from the National Institutes of Health (U.M., NS046456, MH078833; H.C., NS054042), a Christopher Reeve Foundation fellowship (C.S.B.), a National Multiple Sclerosis Society Career Transition Fellowship (H.C.) and a NSF/IGERT 3MT fellowship (T.N., 0549370). Deposited in PMC for release after 12 months.

Supplementary material
Supplementary material for this article is available at http://dev.biologists.org/cgi/content/full/136/16/2717/DC1

References

Belvindrah, R., Graus-Porta, D., Goebbels, S., Nave, K. A. and Muller, U. (2007). Beta1 integrins in radial glia but not in migrating neurons are essential for the formation of cell layers in the cerebral cortex. *J. Neurosci.* **27**, 13854-13865.
Benninger, Y., Colognato, H., Thurnherr, T., Franklin, R. J., Leone, D. P., Atanasoski, S., Nave, K. A., ffrench-Constant, C., Suter, U. and Relvas, J. B. (2006). Beta1-integrin signaling mediates premyelinating oligodendrocyte survival but is not required for CNS myelination and remyelination. *J. Neurosci.* **26**, 7665-7673.
Berti, C., Nodari, A., Wrabetz, L. and Feltri, M. L. (2006). Role of integrins in peripheral nerves and hereditary neuropathies. *Neuromolecular Med.* **8**, 191-204.
Blaess, S., Graus-Porta, D., Belvindrah, R., Radakovits, R., Pons, S., Littlewood-Evans, A., Senften, M., Guo, H., Li, Y., Miner, J. H. et al. (2004). Beta1-integrins are critical for cerebellar granule cell precursor proliferation. *J. Neurosci.* **24**, 3402-3412.
Buttery, P. C. and ffrench-Constant, C. (1999). Laminin-2/integrin interactions enhance myelin membrane formation by oligodendrocytes. *Mol. Cell. Neurosci.* **14**, 199-212.
Cahoy, J. D., Emery, B., Kaushal, A., Foo, L. C., Zamanian, J. L., Christopherson, K. S., Xing, Y., Lubischer, J. L., Krieg, P. A., Krupenko, S. A. et al. (2008). A transcriptome database for astrocytes, neurons, and oligodendrocytes: a new resource for understanding brain development and function. *J. Neurosci.* **28**, 264-278.
Camara, J., Wang, Z., Nunes-Fonseca, C., Friedman, H. C., Grove, M., Sherman, D. L., Komiyama, N. H., Grant, S. G., Brophy, P. J., Peterson, A. et al. (2009). Integrin-mediated axoglial interactions initiate myelination in the central nervous system. *J. Cell Biol.* **185**, 699-712.
Chun, S. J., Rasband, M. N., Sidman, R. L., Habib, A. A. and Vartanian, T. (2003). Integrin-linked kinase is required for laminin-2-induced oligodendrocyte cell spreading and CNS myelination. *J. Cell Biol.* **163**, 397-408.
Colognato, H., Baron, W., Avellana-Adalid, V., Relvas, J. B., Baron-Van Evercooren, A., Georges-Labouesse, E. and ffrench-Constant, C. (2002). CNS integrins switch growth factor signalling to promote target-dependent survival. *Nat. Cell Biol.* **4**, 833-841.
Colognato, H., Ramachandrappa, S., Olsen, I. M. and ffrench-Constant, C. (2004). Integrins direct Src family kinases to regulate distinct phases of oligodendrocyte development. *J. Cell Biol.* **167**, 365-375.
Colognato, H., Galvin, J., Wang, Z., Relucio, J., Nguyen, T., Harrison, D., Yurchenco, P. D. and ffrench-Constant, C. (2007). Identification of dystroglycan as a second laminin receptor in oligodendrocytes, with a role in myelination. *Development* **134**, 1723-1736.
Corley, S. M., Ladiwala, U., Besson, A. and Yong, V. W. (2001). Astrocytes attenuate oligodendrocyte death in vitro through an alpha(6) integrin-laminin-dependent mechanism. *Glia* **36**, 281-294.
Farina, L., Morandi, L., Milanesi, I., Ciceri, E., Mora, M., Moroni, I., Pantelioni, C. and Savoiardo, M. (1998). Congenital muscular dystrophy with merosin deficiency: MRI findings in five patients. *Neuroradiology* **40**, 807-811.
Flores, A. I., Narayanan, S. P., Morse, E. N., Shick, H. E., Yin, X., Kidd, G., Avila, R. L., Kirschner, D. A. and Macklin, W. B. (2008). Constitutively active Akt induces enhanced myelination in the CNS. *J. Neurosci.* **28**, 7174-7183.
Fraser, M. M., Bayazitov, I. T., Zakharenko, S. S. and Baker, S. J. (2008). Phosphatase and tensin homolog, deleted on chromosome 10 deficiency in brain causes defects in synaptic structure, transmission and plasticity, and myelination abnormalities. *Neuroscience* **151**, 476-488.
Frost, E. E., Buttery, P. C., Milner, R. and ffrench-Constant, C. (1999). Integrins mediate a neuronal survival signal for oligodendrocytes. *Curr. Biol.* **9**, 1251-1254.
Graus-Porta, D., Blaess, S., Senften, M., Littlewood-Evans, A., Damsky, C., Huang, Z., Orban, P., Klein, R., Schittny, J. C. and Muller, U. (2001). Beta1-class integrins regulate the development of laminae and folia in the cerebral and cerebellar cortex. *Neuron* **31**, 367-379.
Hoshina, N., Tezuka, T., Yokoyama, K., Kozuka-Hata, H., Oyama, M. and Yamamoto, T. (2007). Focal adhesion kinase regulates laminin-induced oligodendroglial process outgrowth. *Genes Cells* **12**, 1245-1254.
Jones, K. G., Morgan, G., Johnston, H., Tobias, V., Ouvrier, R. A., Wilkinson, I. and North, K. N. (2001). The expanding phenotype of laminin alpha2 chain (merosin) abnormalities: case series and review. *J. Med. Genet.* **38**, 649-657.
Lee, K. K., de Repentigny, Y., Saulnier, R., Rippstein, P., Macklin, W. B. and Kothary, R. (2006). Dominant-negative beta1 integrin mice have region-specific myelin defects accompanied by alterations in MAPK activity. *Glia* **53**, 836-844.
Lukashev, M. E., Sheppard, D. and Pytela, R. (1994). Disruption of integrin function and induction of tyrosine phosphorylation by the autonomously expressed beta 1 integrin cytoplasmic domain. *J. Biol. Chem.* **269**, 18311-18314.
Milner, R. and ffrench-Constant, C. (1994). A developmental analysis of oligodendroglial integrins in primary cells: changes in alpha v-associated beta subunits during differentiation. *Development* **120**, 3497-3506.
Milner, R., Edwards, G., Streuli, C. and ffrench-Constant, C. (1996). A role in migration for the alpha V beta 1 integrin expressed on oligodendrocyte precursors. *J. Neurosci.* **16**, 7240-7252.
Milner, R., Frost, E., Nishimura, S., Delcommenne, M., Streuli, C., Pytela, R. and ffrench-Constant, C. (1997). Expression of alpha vbeta3 and alpha vbeta8 integrins during oligodendrocyte precursor differentiation in the presence and absence of axons. *Glia* **21**, 350-360.
Nishiyama, A., Lin, X. H., Giese, N., Heldin, C. H. and Stallcup, W. B. (1996). Co-localization of NG2 proteoglycan and PDGF alpha-receptor on O2A progenitor cells in the developing rat brain. *J. Neurosci. Res.* **43**, 299-314.
Raff, M. C., Durand, B. and Gao, F. B. (1998). Cell number control and timing in animal development: the oligodendrocyte cell lineage. *Int. J. Dev. Biol.* **42**, 263-267.
Relvas, J. B., Setzu, A., Baron, W., Buttery, P. C., LaFlamme, S. E., Franklin, R. J. and ffrench-Constant, C. (2001). Expression of dominant-negative and chimeric subunits reveals an essential role for beta1 integrin during myelination. *Curr. Biol.* **11**, 1039-1043.
Richardson, W. D., Kessaris, N. and Pringle, N. (2006). Oligodendrocyte wars. *Nat. Rev. Neurosci.* **7**, 11-18.
Scherer, S. S., Braun, P. E., Grinspan, J., Collarini, E., Wang, D. Y. and Kamholz, J. (1994). Differential regulation of the 2′,3′-cyclic nucleotide 3′-phosphodiesterase gene during oligodendrocyte development. *Neuron* **12**, 1363-1375.
Schmid, A. C., Byrne, R. D., Vilar, R. and Woscholski, R. (2004). Bisperoxovanadium compounds are potent PTEN inhibitors. *FEBS Lett.* **566**, 35-38.
Sherman, D. L. and Brophy, P. J. (2005). Mechanisms of axon ensheathment and myelin growth. *Nat. Rev. Neurosci.* **6**, 683-690.
Simons, M. and Trajkovic, K. (2006). Neuron-glia communication in the control of oligodendrocyte function and myelin biogenesis. *J. Cell Sci.* **119**, 4381-4389.
Simons, M. and Trotter, J. (2007). Wrapping it up: the cell biology of myelination. *Curr. Opin. Neurobiol.* **17**, 533-540.
Stephens, L. E., Sutherland, A. E., Klimanskaya, I. V., Andrieux, A., Meneses, J., Pedersen, R. A. and Damsky, C. H. (1995). Deletion of beta 1 integrins in mice results in inner cell mass failure and peri-implantation lethality. *Genes Dev.* **9**, 1883-1895.
Sulis, M. L. and Parsons, R. (2003). PTEN: from pathology to biology. *Trends Cell Biol.* **13**, 478-483.
Tiwari-Woodruff, S. K., Buznikov, A. G., Vu, T. Q., Micevych, P. E., Chen, K., Kornblum, H. I. and Bronstein, J. M. (2001). OSP/claudin11 forms a complex with a novel member of the tetraspanin super family and beta1 integrin and regulates proliferation and migration of oligodendrocytes. *J. Cell Biol.* **153**, 295-305.
Tohda, C., Nakanishi, R. and Kadowaki, M. (2007). Learning deficits and agenesis of synapses and myelinated axons in phosphoinositide-3 kinase-deficient mice. *Neurosignals* **15**, 293-306.
Zhu, X., Bergles, D. E. and Nishiyama, A. (2008). NG2 cells generate both oligodendrocytes and gray matter astrocytes. *Development* **135**, 145-157.

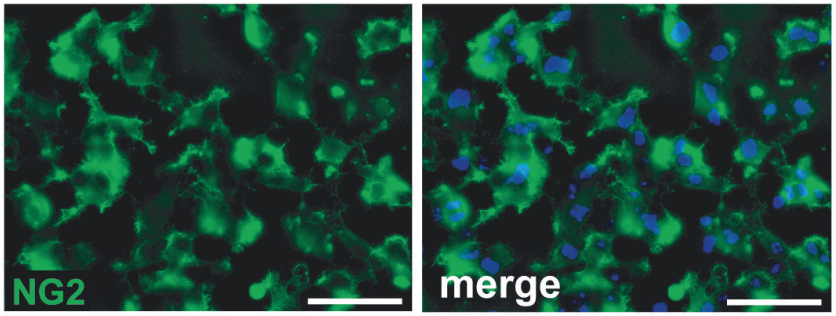
A
NG2
merge

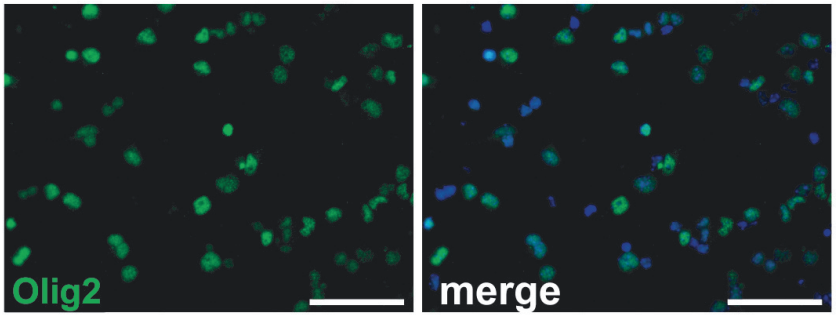
B
Olig2
merge

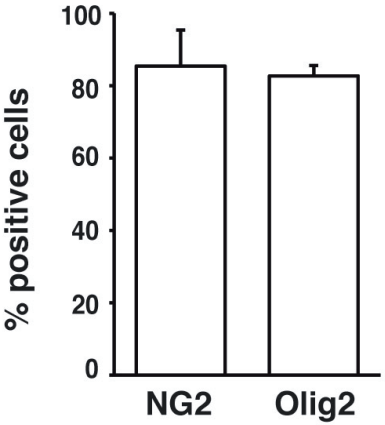
C
% positive cells
100
80
60
40
20
0
NG2
Olig2

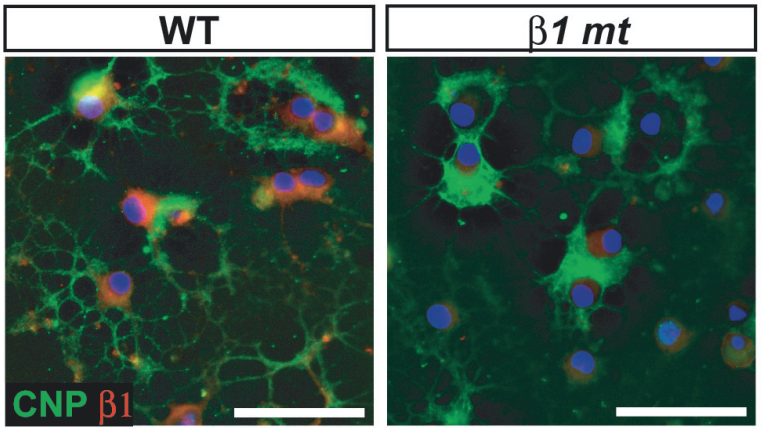
D
WT
β1 mt
CNP β1

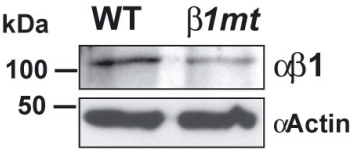
E
kDa
WT
β1mt
100
50
αβ1
αActin

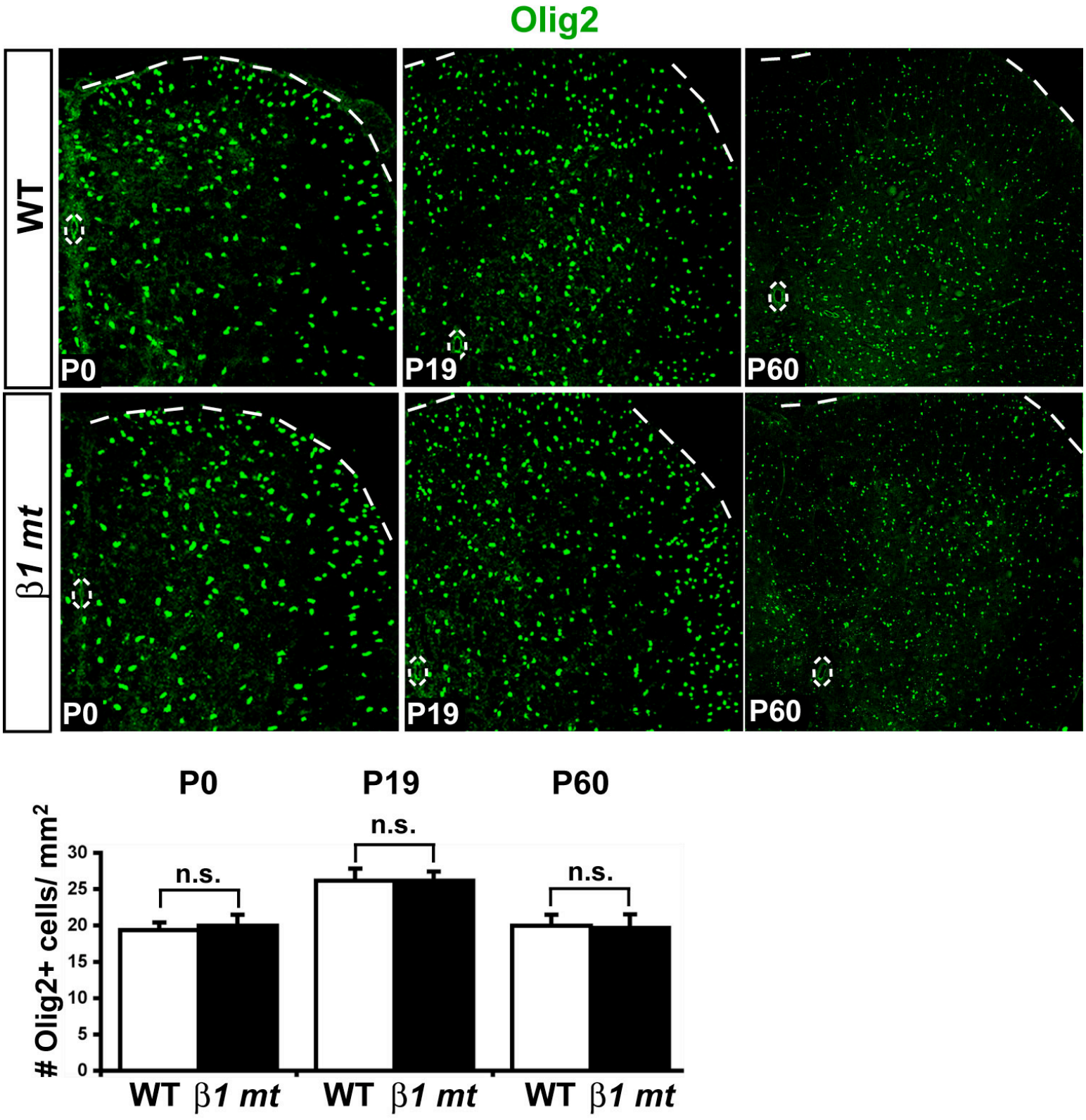
Olig2
WT
β1 mt
P0
P19
P60
P0
P19
P60
P0
P19
P60
n.s.
n.s.
n.s.
Olig2+ cells/ mm2
30
25
20
15
10
5
0
WT
β1 mt
WT
β1 mt
WT
β1 mt

Tunel Topro-3

WT

β1 mt

P0

P19

P60

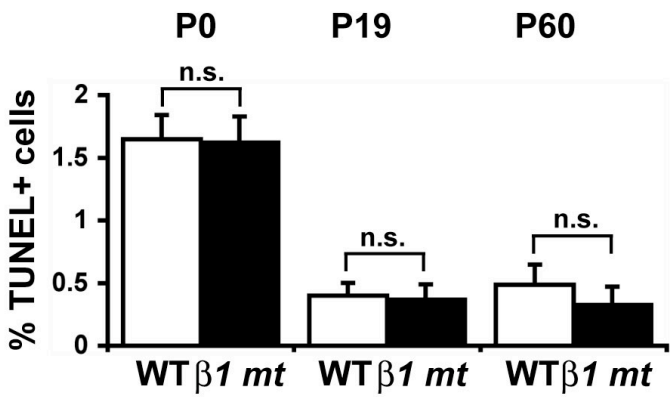

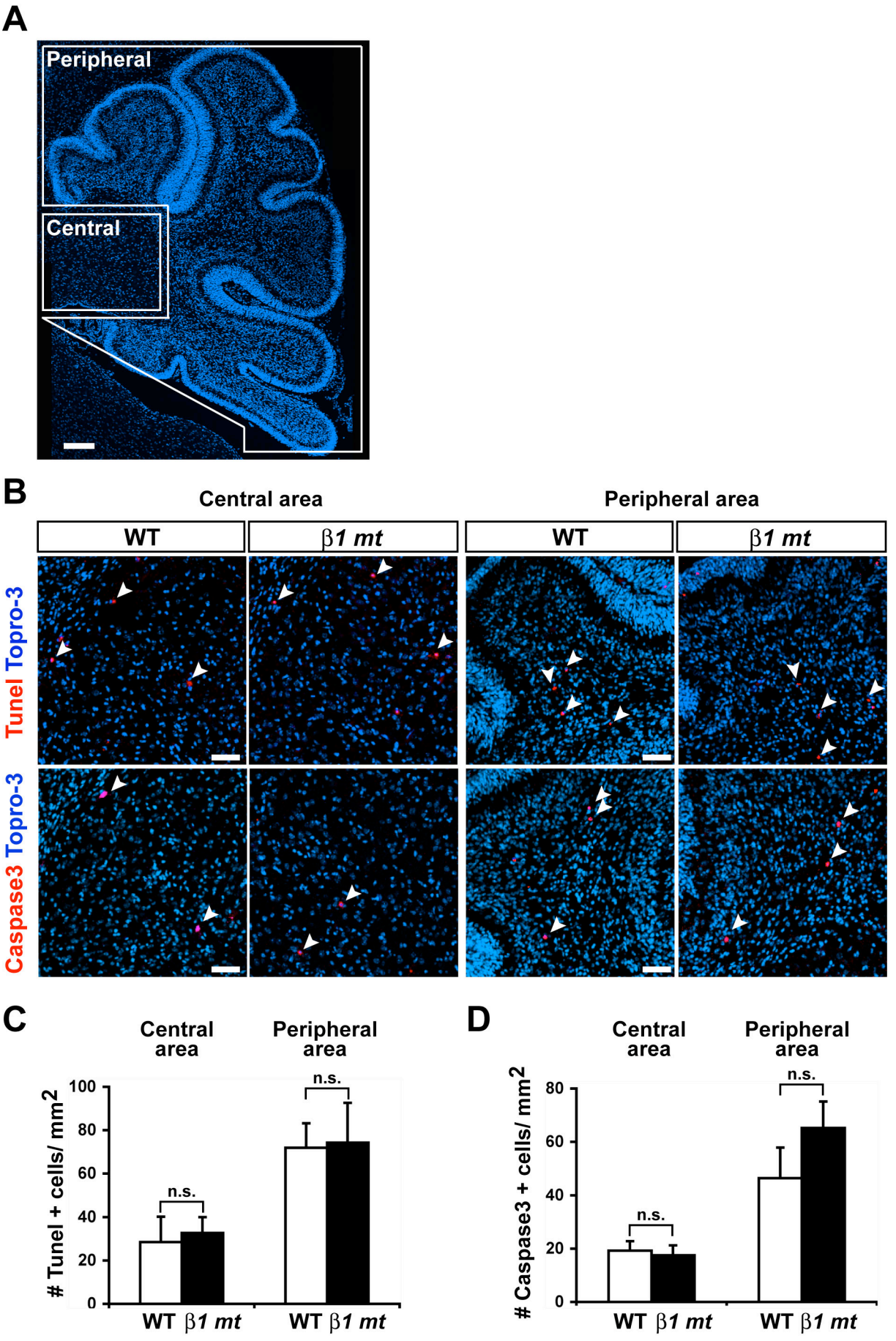
A
Peripheral
Central
B
Central area
Peripheral area
WT
β1 mt
WT
β1 mt
Tunel Topro-3
Caspase3 Topro-3
C
Central area
Peripheral area
Tunel + cells/ mm2
100
80
60
40
20
0
n.s.
n.s.
WT β1 mt
WT β1 mt
D
Central area
Peripheral area
Caspase3 + cells/ mm2
80
60
40
20
0
n.s.
n.s.
WT β1 mt
WT β1 mt

A

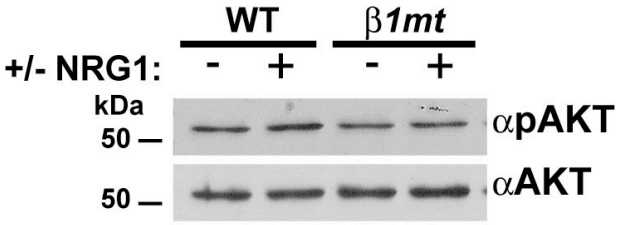
WT
β1mt
+/- NRG1:
-
+
-
+
kDa
50
αpAKT
50
αAKT

B

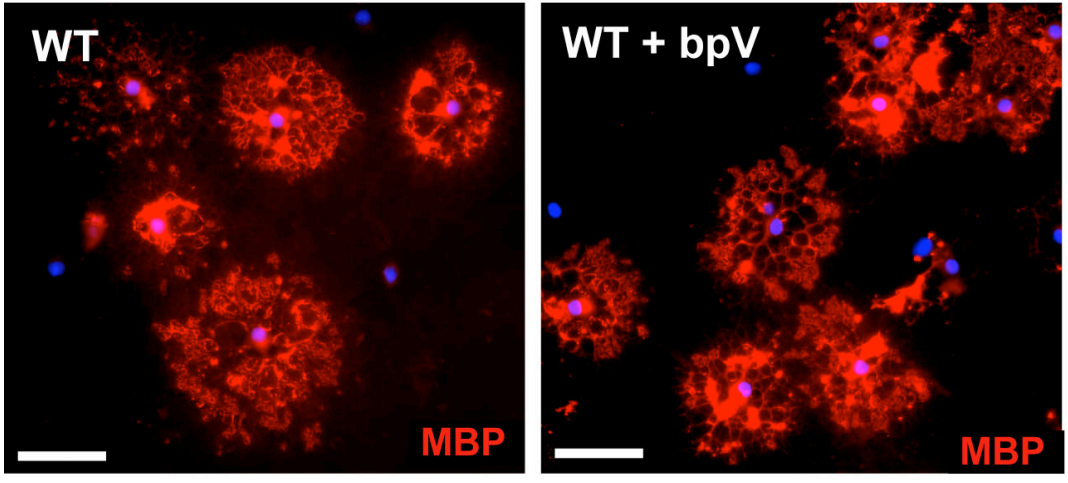
WT
MBP
WT + bpV
MBP

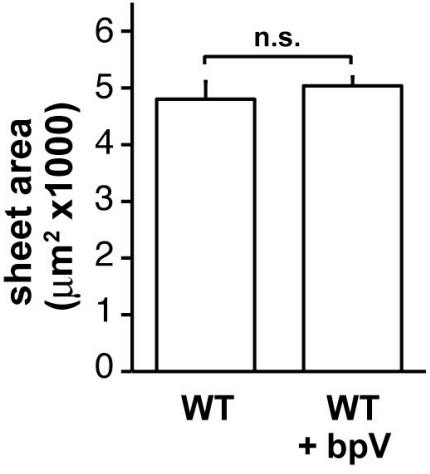
n.s.
sheet area
(μm² x1000)
0
1
2
3
4
5
6
WT
WT
+ bpV

Table S1. Decreased g-ratios in CNS axons of *Itgb1-CNSko* and *Itgb1-OL-ko* mice

		G-ratio		
Fiber	Axon diameter (μm)	WT (*n*)	MT (*n*)	Mann-Whitney
Spinal cord	0.6-0.7	0.714±0.005 (128)	0.708±0.008 (136)	*P*=0.5533
	0.71-1.1	0.741±0.003 (488)	0.754±0.003 (519)	***P*=0.0023
	1.11-2.5	0.765±0.002 (594)	0.794±0.002 (810)	****P*=0.0001
	>2.5	0.787±0.003 (278)	0.818±0.003 (313)	****P*=0.0001
Optic nerves	0.6-1.0	0.756±0.002 (579)	0.758±0.003 (483)	*P*=0.5783
	1.1-1.5	0.798±0.002 (447)	0.805±0.003 (329)	**P*=0.0422
	1.51-2.0	0.820±0.003 (158)	0.835±0.004 (129)	***P*=0.0017
	>2.1	0.828±0.005 (49)	0.856±0.004 (69)	****P*=0.0001
Cerebellum	0.6-0.7	0.717±0.011 (33)	0.731±0.019 (17)	*P*=0.4892
	0.71-1.2	0.741±0.006 (93)	0.758±0.007 (88)	*P*=0.0584
	>1.2	0.763±0.009 (30)	0.801±0.054 (31)	***P*=0.005
Spinal cord (*Ng2-Cre*)	0.6-0.7	0.745±0.007 (72)	0.768±0.007 (33)	*P*=0.0532
	0.71-1.1	0.759±0.003 (290)	0.785±0.003 (173)	****P*=0.0001
	1.11-2.5	0.762±0.003 (369)	0.783±0.003 (256)	****P*=0.0001
	>2.5	0.793±0.002 (206)	0.799±0.003 (129)	*P*=0.1041

G-ratio values for fibers grouped by axon diameter in spinal cords, optic nerves and cerebellum from *Itgb1* conditional knockout mice (MT) and WT littermates derived using nestin-*Cre*, and in mouse spinal cords derived using *Ng2-Cre*. Values are shown as mean±s.e.m. The number of scored fibers in each group is also shown in parentheses. Statistical significance calculated using Mann-Whitney (rank sum) test is shown. In the spinal cords, optic nerves and cerebellum of mutant mice derived using nestin-*Cre* there was a significant increase in the g-ratio in the larger caliber fibers (spinal cords, cerebellum: *n*=3 WT and *n*=3 *Itgb1-CNSko* animals; optic nerves: *n*=2 WT and *n*=2 *Itgb1-CNSko* animals). In the spinal cords of mutant mice derived using *Ng2-Cre* there was a significant increase in the g-ratio in the majority of fibers (429 out of 591) with axons between 0.71 and 2.5 μm in diameter (spinal cords *Ng2-Cre*: *n*=2 WT and *n*=2 *Itgb1-OL-ko* animals).